Load-specific variant generation of bead cross sections in sheet metal components by unidirectional carbon fibre reinforcement

M Ott[1]*, P Haberkern[2], M Gruber[1], C Hartmann[1], T Risch[1], C Wunderling[3], A Albers[2] and W Volk[1]

[1] Chair of Metal Forming and Casting, Technical University of Munich, Walther-Meissner-Strasse 4, 85748 Garching, Germany

[2] Institute of Product Engineering, Karlsruhe Institute of Technology, Kaiserstrasse 10, 76131 Karlsruhe, Germany

[3] Institute for Machine Tools and Industrial Management, Technical University of Munich, Boltzmannstrasse 15, 85478 Garching, Germany

*michael.ott@utg.de

Abstract. Beads are widely used to stiffen sheet metal components subjected to bending loads. Often, these bead-stiffened parts are used in product variants that differ significantly in the amount of acting loads. Lamination of unidirectional carbon fibre reinforced plastic (UD-CFRP) on the top flange area of individual beads represents a method for further increasing weight-specific stiffness: By varying the number of plies, a specifically configured component is obtained for each of the load cases. As a result, no changes to the forming tools are necessary and a minimum amount of the UD-CFRP material is required. In this work, a complete manufacturing process for a fibre reinforced bead was developed: First, a bead cross section geometry with an adapted top flange area to accommodate the UD-CFRP plies was designed and stamped into pre-stretched sheet samples of DX56 steel. Subsequently, the suitability of several surface pre-treatment processes to achieve sufficient bond strength of the composite bead was experimentally investigated and the UD-CFRP plies were applied by lamination. Final bending tests quantified the achievable stiffening effect of the investigated bead variants, showing a significant increase of the maximum supportable load compared to the standard non-reinforced cross-section.

1. Introduction

In order to meet customer-specific requirements, products appear in multiple variants, often showing high mass differences. For example, in the automotive industry these can amount to more than 500 kg within a series [1]. A uniform design of individual product components with respect to the peak-loaded variant leads to over-dimensioning of the lower-loaded variants, which counteracts cost and lightweight design objectives. One possible solution is to create variants at the component level. When sheet metal forming processes are used, however, cost-intensive adjustments to the forming tools are necessary. This makes the design variants uneconomical, especially for parts with low volumes [2]. For components subjected predominantly to bending loads, a hybrid material approach for generating cost-

effective manufacturable component variants is investigated: First, a beaded base component is created. Subsequently, load-specific component variations can be derived by locally applying a variable number of plies of unidirectional carbon fibre reinforced plastic (UD-CFRP) to the bead cross section.

2. State of the art

The insertion of beads represents a method of structural lightweight design and an extensive analysis of various bead patterns was performed in [3]. The magnitude of the reinforcing effect depends both on the geometrical parameters of the bead cross-section as well as on the arrangement of the beads in the component. For the resulting topology optimization problem, a method was developed that couples a bead optimization based on main bending stress trajectories with forming simulation to determine bead patterns while considering manufacturability [4]. With regard to the design of reinforced hybrid beads, the anisotropic mechanical properties of FRP impact the stiffening effect. For long fibre reinforced plastic injection moulded components, the influence on the stiffness of beads resulting from a specific determination of the fibre orientations has already been shown [5]. In addition, hybrid sheet metal components that combine sheet metal and FRP are already being used in the automotive and aerospace industry. For example, the hybrid material GLARE (glass fibre reinforced aluminium) that consists of alternating layers of aluminium foil and glass fibre laminate is used for the fuselage of passenger aircraft [6]. In order to prepare the lamination of fibre reinforced plastic onto metal sheets, various surface pre-treatments can be performed on the metal sheet. The objective is to improve the resulting bond strength by increasing the effective surface area. An overview of the mechanisms influencing adhesion and a description of the processes used such as sand blasting, plasma etching and application of adhesion promoters are detailed in [7].

3. Approach

The aim of this work is to show the manufacturability of the reinforced hybrid beads and to verify the predicted reinforcement effect for different reinforcement variants. For this purpose, a complete chain of the design and manufacturing process is implemented: To accommodate the local UD-CFRP-reinforcement, a matched trapezoidal bead is designed based on analytical considerations and stamped into pre-stretched sheets. Subsequently, several surface pre-treatment processes for achieving sufficient bond strength of the hybrid component are compared experimentally. Finally, the achievable increase in bending stiffness is quantified in three-point bending tests.

3.1. Analytical principle of the reinforcing effect due to hybrid beads

According to Bernoulli's elastic beam theory, the bending stiffness of a profiled beam is the product of the modulus of elasticity E and the area moment of inertia I. By analogy, the insertion of beads in sheet metal components leads to an increase of the bending stiffness in the direction of the bead axis that results from the increase in the area moment of inertia. For a trapezoidal bead stamped into a sheet with the modulus of elasticity E_{sheet}, to which reinforcements made of an UD-FRP material with the modulus of elasticity $E_{\mathrm{UD-FRP}}$ in the direction of the fibres are applied locally, a total bending stiffness $(E \cdot I)_{\mathrm{total}}$ is obtained against a static bending load acting on the bead for an arbitrary given coordinate system, cf. Figure 1:

$$(E \cdot I)_{total} = E_{sheet} \cdot \left(I_{sheet,GC} + I_{sheet,Steiner}\right) + E_{UD-FRP} \cdot \left(I_{UD-FRP,GC} + I_{UD-FRP,Steiner}\right) \quad (1)$$

For both components, the area moment of inertia consists of a portion I_{GC} around the respective area's geometric centre (GC) with vertical position z_{GC} and a portion I_{Steiner} according to the parallel axis theorem (Steiner's theorem):

$$I_{GC} = \int_A z^2 \, dA \quad (2)$$

$$I_{Steiner} = (z_{GC} - z_{NF})^2 \cdot A \quad (3)$$

z_{NF} denotes the vertical position of the neutral fibre (NF) of the hybrid bead and A denotes the cross section of the respective component:

$$z_{NF} = \frac{E_{sheet} \cdot \int_{A_{sheet}} z\, dA + E_{UD-FRP} \cdot \int_{A_{UD-FRP}} z\, dA}{E_{sheet} * A_{sheet} + E_{UD-FRP} \cdot A_{UD-FRP}} = \frac{E_{sheet} \cdot z_{GC,sheet} \cdot A_{sheet} + E_{UD-FRP} \cdot z_{GC,UD-FRP} \cdot A_{UD-FRP}}{E_{sheet} \cdot A_{sheet} + E_{UD-FRP} \cdot A_{UD-FRP}} \quad (4)$$

For a fixed quantity of UD-CFRP, the Steiner portion can be increased as a contribution to lightweight design targets. For this purpose, the UD-CFRP reinforcement is positioned as far from the neutral fibre as possible. In the bead geometry, the top flange area was therefore selected as the location of the reinforcement, as shown in Figure 1. When the fibres in CFRP are subjected to compressive loads, micro-buckling can occur. Because of this, the hybrid material GLARE is used in aircraft construction in the areas of the fuselage that are predominantly loaded by tensile forces [8]. Thus, for components loaded by static bending loads, it emerges as a design guideline to align the beads in such a way that the top flange area laminated with the UD-CFRP is loaded by tensile stresses along the bead axis. The resulting stress profile through the cross section is plotted for the two subcomponents in Figure 1.

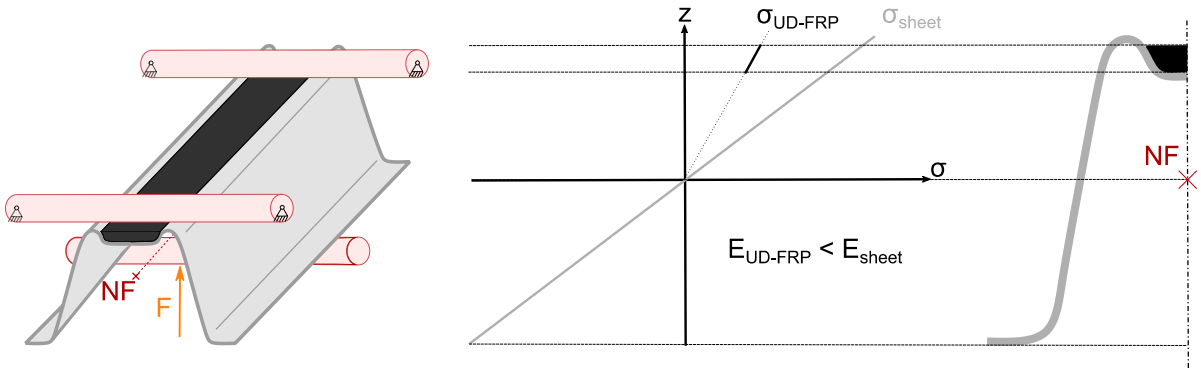

Figure 1. Load case of the hybrid bead with the top flange area loaded by tensile stresses under static three-point bending load due to the force F.

3.2. Design and manufacturing of the basic bead

In a first step of the experimental implementation, a trapezoidal bead cross section geometry to be stamped was designed. In order to increase the bonding surface of the UD-CFRP, a channel-shaped recess was brought into the top flange area. In addition, this structure in conjunction with the UD-CFRP increases the buckling stiffness of the top flange area, allowing wider beads to be used. The maximum bead height that can be achieved is limited by the occurrence of tearing during bead stamping. Therefore, a pronounced stiffening effect results when a sheet material with high formability and thus a high achievable bead height is combined with a reinforcing material with a high modulus of elasticity. With regard to lightweight design targets for beaded components, its formability must also be taken into account in addition to the density of the sheet material. In the following investigations, the sheet material DX56+Z100 was therefore selected as a galvanized deep-drawing steel that exhibits good formability, with a sheet thickness of 1 mm and a zinc coating thickness of 7 µm. This is also widely used for the production of car body parts and is therefore of industrial relevance for the variant designs under consideration. In the sheet metal components to be provided with beads described as the application target, the sheet is subjected to pre-stretching by the die and blank holder geometry before the actual stamping of the bead. Depending on the local extent of the pre-stretching, different heights of the individual beads can therefore be produced. The influence of different pre-strain states on the stamping of beads has already been investigated using both a numerical simulation model and experimentally in

[8]: For this purpose, the forming tool geometry developed in [9] was used to generate different pre-strain states and was supplemented with inserts for the subsequent stamping of the bead. Thereby, the strain state in the sheet metal area in which the bead is stamped can be defined by adjusting the blank geometry. This approach was adopted and two inserts, marked in colour in Figure 2(a) and (b), were inserted into the tool geometry according to [9] to form the bead geometry. For the subsequent production of the beads, the blank geometries shown in Figure 2(d) and (e) were selected. The manufacturability with regard to tear formation was verified by means of a finite element simulation model of the entire forming process in Autoform R8, as shown in Figure 2(c). Using a Dieffenbacher DXU 320 B double-acting hydraulic press, the production of the beads was possible without the occurrence of tearing for both of the used blank geometries.

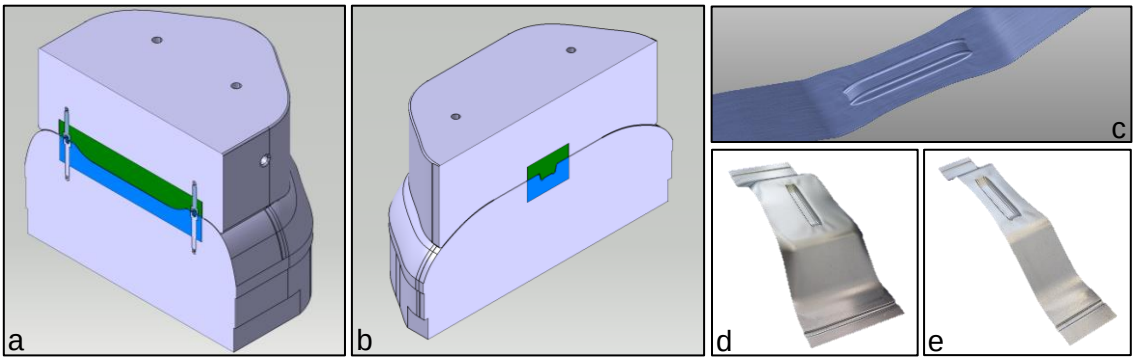

Figure 2. Sectionals views (a) and (b) of the upper and lower die of the forming tool with colour marked inserts (blue/green) for bead creation from the CAD model. Isometric view of the sheet geometry with the centrally inserted bead generated from the Autoform simulation model (c) compared to the manufactured parts (d and e).

3.3. Surface pre-treatment to enhance bond strength of the hybrid beads

For the hybrid beads, the goal was defined as achieving such a high bond strength that delamination at the bond interface would not be the limiting failure mechanism under an applied bending load. Instead, failure within the UD-CFRP or plastic deformation of the sheet would occur beforehand. In order to achieve this, several possible processes were experimentally applied to the top flange area of the stamped beads: chemical etching with hydrochloric acid and nitric acid, sandblasting with two different configurations and two types of laser structuring. The acids were present in 10 % aqueous (hydrochloric acid) and 10 % alcoholic (nitric acid) solutions, and exposure times of 90 s and 300 s were investigated. Sandblasting was investigated on a SAPI T-REX 140 using corundum sand as the blasting medium and both pressure blasting and injector blasting were performed with an approximate processing time of 30 s. The laser radiation was used to generate a triple bi-directional and a circular beam oscillation surface pattern according to two of the strategies detailed in [10]. A single-mode fibre laser IPG YLR 3000-SM was used for both methods. For the structuring of the top flange area of the bead, a time span of 11.6 s for the triple bi-directional pattern and 2.1 s for the circular beam oscillation pattern was required. Following the surface treatment, a Keyence VK-X100 confocal 3D laser scanning microscope was used to image the surface structure and to measure the surface roughness of the manufactured variants. Compared to the untreated reference configuration, the surface structures shown in Figure 3 and the effect on the mean arithmetic height (Sa) shown in Figure 4 were obtained. The standard deviation for the error indicators was calculated from three measurements for each bar. The smallest effect on the surface roughness was achieved with chemical etching. Therefore, only the other two process types were used for the subsequent investigations. For the two laser structuring processes, a similarly pronounced effect on Sa as in [10] was obtained for the DX56 steel used here. For sandblasting, a stronger effect can be seen with the pressure blasting variant in comparison with the injection blasting variant.

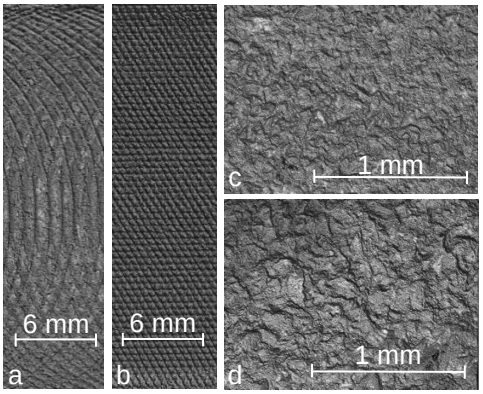

Figure 3. Images of the sheet surface after laser structuring (a: circular beam oscillation, b: triple bi-directional) and after sandblasting (c: pressure blasting, d: injector blasting) generated on a confocal laser microscope at 10x magnification

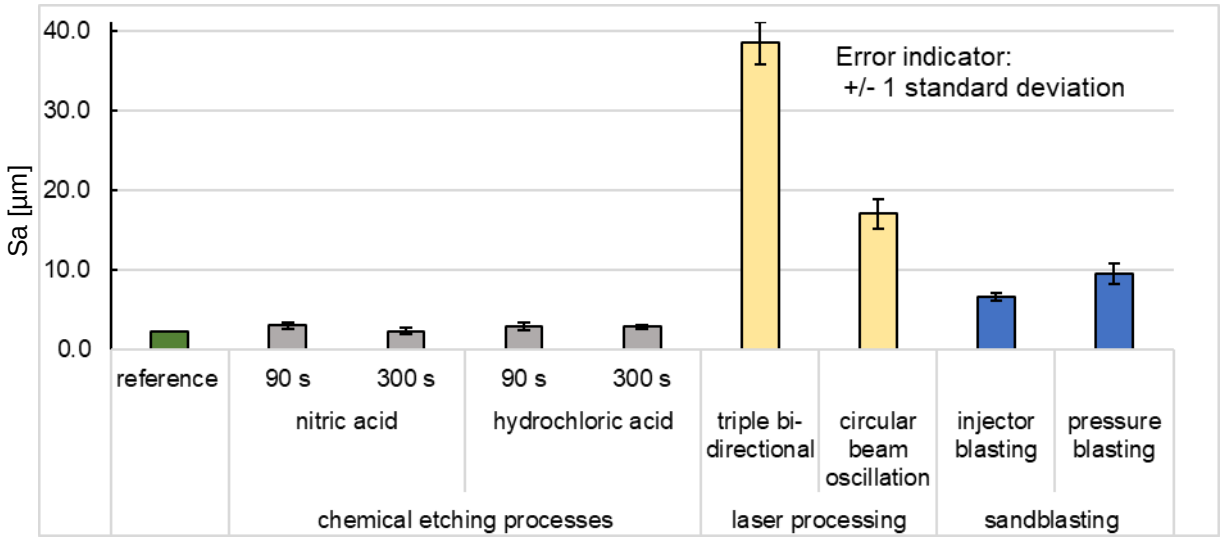

Figure 4. Mean arithmetic height Sa according to ISO 25178 after surface pre-treatment processing.

3.4. Manufacturing of the hybrid beads

In the next step, several variants of the hybrid bead were manufactured. Therefore, UD-CFRP was laminated onto the surface-pre-treated top flange area of the formed beads. In an initial series of tests, reinforcement by vacuum-assisted resin infusion was performed on one sample of both of the two sand-blasted bead variants to investigate the general feasibility of the laminating process. For this purpose, the Sigrafil C T50-4.0/240-E10 fibres and a matrix composed of the Ebalta AH 140 epoxy resin with the Ebalta TC 90-2 hardener were used. In a second series, with regard to subsequent industrial applications, pre-impregnated fibre bundles were deposited using an AFP (automated fibre placement)-unit and then laminated onto the laser-structured beads. In this case, Hexcel AS7 fibres were used with the Hexcel 8552 epoxy resin matrix. In order to be able to compare the influence of different reinforcement variants on achievable stiffness, 3 plies with a material-specific nominal cured ply thickness of 0.35 mm were used for the hand-laminated beads and one specimen with 4 plies and two specimens with 12 plies with a nominal cured ply thickness of 0.13 mm were used for the AFP-based variant in each case.

For both production variants, multi-stage cleaning of the pre-treated sheet surface was conducted before lamination: First, an ultrasonic bath with propanol as the ambient medium was performed for 5 min, followed by another 5 min ultrasonic bath with acetone, and then rinsing with deionised water. In the next step, the difference between the two variants is that for the first variant, only the fibres are

applied and the resin-hardener mixture infiltrates the fibres later after the vacuum has been built up, while in the second variant, the pre-impregnated fibres are applied directly onto the sheet. For a possible implementation of the hybrid beads in industrially manufactured components, the shorter cycle time and the higher degree of automation achievable represent advantages for the latter variant. After a subsequent vacuum build-up in a foil pocket applied around the laminated area, 24 hours of initial cure at room temperature and 16 hours post-cure at 80 °C were performed for the first variant. For the second production variant, a curing procedure with a stepped temperature increase to a maximum at 180 °C with a duration of 150 minutes was performed. In total, the two processes were able to produce the hybrid beads, whose cross sections are shown in Figure 5(a) and (b). In Figure 5(c) and (d), the characteristic microstructure at the interface of the two components due to the sand blasting and laser structuring surface pre-treatments can be seen.

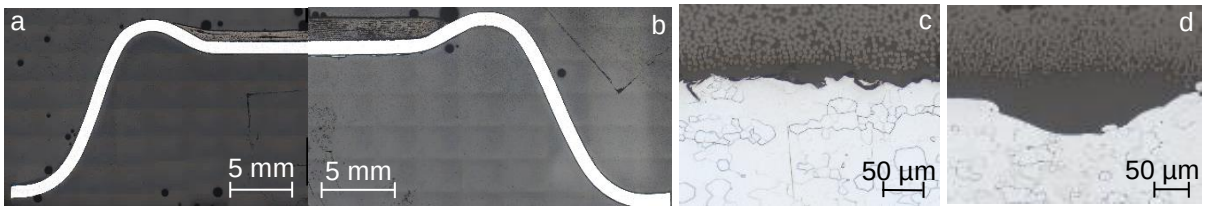

Figure 5. Micrographs of the specimen cross sections, created after performing the three-point bending tests, cf. section 5: Manual laminated, 3 plies, pressure blasted sheet surface (a), AFP-based-laminate, 12 plies, laser structured surface (circular beam oscillation) (b). Detail of the interface between sheet metal and UD-CFRP for pressure-blasted (c) and laser-structured (circular beam oscillation) sheet surface (d).

4. Experimental quantification

The three-point bending test was chosen to quantify the achievable additional stiffening effect of the manufactured configurations of UD-CFRP. The loading condition in this test is analogous to the loading of a bead aligned along the principal bending stress direction in the sheet metal components defined as the application target. For this purpose, the bead was cut out of the formed base surface with a length of 225 mm and a width of 78 mm. With this geometry, the bending tests were performed on a ZwickRoell 1484 universal testing machine with the specimen orientation shown in Figure 6, so that tensile stresses act in the top flange area of the bead (cf. Figure 1). The distance between the two lower cuboid supports was 120 mm, the radius of the upper centre punch was 11 mm and the punch was moving at a speed of 10 mm/min during the testing procedure. Figure 7 shows the force-displacement curves for a non-reinforced reference geometry, two beads reinforced with hand laminate and three beads reinforced with the fibres deposited in the AFP process. The supportable load increases for both manufacturing variants: For the manual laminated variant, an increase in the maximum force by 18.8 %, and for the AFP-version using 12 plies, an increase of 6.14 % compared to the non-reinforced reference configuration. In the force-displacement measurements, a stepped decrease in force occurs for the specimens reinforced with 12 plies and those reinforced with 3 plies, corresponding to two damage mechanisms occurring in the UD-CFRP. Failure of the UD-CFRP layer occurred both for the hand-laminated specimens, which were pre-treated with the two sandblasting processes, and for the AFP specimens, which were pre-treated with the two laser processes, by fibre breakage after the sheet had already undergone significant plastic deformation. For the bead reinforced with 4 plies, fibre breakage of the UD-CFRP occurred only in the edge area, which is elevated due to the bead geometry. This behaviour is in agreement with the assumption that strain increases with greater vertical distance from the neutral fibre. In the case of the AFP specimens, a cohesive failure due to detachment of individual UD-CFRP plies can additionally be seen, which also initiated after the onset of plastic deformation of the sheet. However, a thin UD-CFRP layer on the sheet surface shows that also no adhesive failure occurs at the interface between sheet and UD-CFRP for the pre-treatment with laser structuring. The use of an additional adhesion promoter, such as a diamond-like carbon (DLC)-layer used by [9] for joining hybrid sheets, can thus be dispensed with for both surface pre-treatment processes.

Figure 6. Test performance of the three-point bending test.

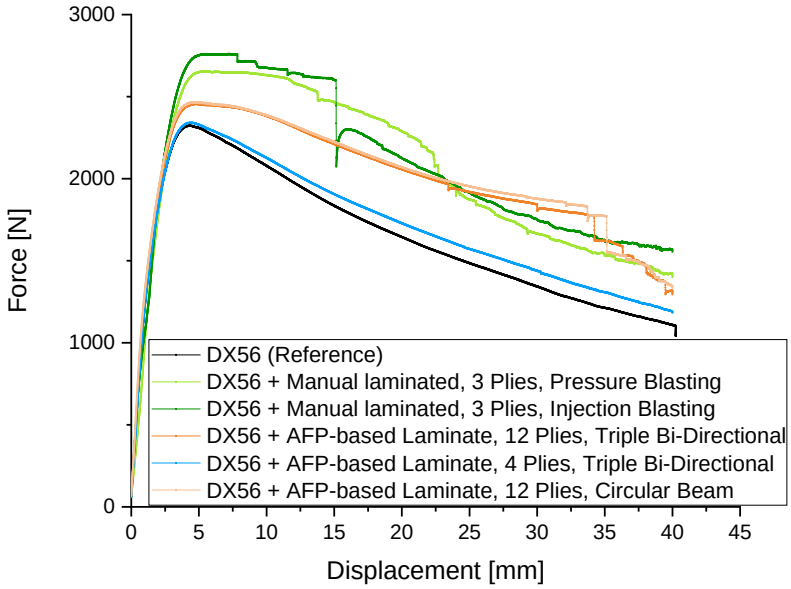

Figure 7. Force-displacement-measurements of the non-reinforced reference bead and the hybrid beads during the three-point bending test.

5. Summary and Outlook

The feasibility of stiffening beaded components with UD-carbon fibres in the top flange area was demonstrated for the DX56/UD-CFRP material combination. Thus, the maximum force in the three-point bending test for the variant could be increased using both the manual laminated and the AFP-based manufacturing processes. By utilizing the parallel axis theorem and the anisotropic material properties of the UD fibres, a stiffening effect was achieved with a relatively small amount of CFRP. This allows the material and manufacturing costs for lamination to be kept within reasonable limits in an industrial implementation. Furthermore, the additional stiffening correlates with the number of applied UD-CFRP plies, thus fulfilling a necessary condition to produce load-specific component variants. Both the sandblasting and laser structuring processes were able to achieve sufficient bond strength between the sheet and the UD-CFRP, which can prevent early delamination of the hybrid bead at low applied forces. The shortest processing times were achieved with the laser structuring processes. The following steps are necessary to enable transferability to industrial applications: The results regarding the reinforcing effect of the UD-CFRP should be coupled with the optimization method developed by [4] to determine load specific, locally reinforced bead patterns. Furthermore, an application of the beads with automated, direct lamination of the fibres onto the formed sheet metal component should be investigated experimentally to further reduce manufacturing time. In addition, the procedure can be adapted to various UD fibre reinforced materials, such as glass or aramid fibre reinforced plastic. This means that the design of the component variants may also take into account the specific target costs accepted for weight saving in various fields of application. A desired stiffening effect can predictably be achieved with this approach with glass fibres compared to carbon fibres at lower additional cost, but with a higher component mass.

Acknowledgements

The authors gratefully acknowledge the German Research Foundation (Deutsche Forschungsgemeinschaft, DFG) for supporting this work carried out within the framework of the collaborative research project 431606085 (VO 1487/51-1). Moreover, the authors want to thank Manuel Arrillaga Tamez (Fraunhofer Institute for Casting, Composite and Processing Technology IGCV) for his support during the lamination and curing of the UD-CFRP.

References

[1] Ellenrieder G, Friedrich H E and Kienzle S 2013 Leichtbaukonzepte für heute und morgen *Leichtbau in der Fahrzeugtechnik (ATZ / MTZ-Fachbuch)* ed H E Friedrich (Wiesbaden, s.l.: Springer Fachmedien Wiesbaden) pp 773–826

[2] Hartmann C, Opritescu D and Volk W 2019 An artificial neural network approach for tool path generation in incremental sheet metal free-forming *J Intell Manuf* **30** 757–70

[3] Schwarz D 2002 *Auslegung von Blechen mit Sicken (Sickenatlas)* (Forschungsvereinigung Automobiltechnik e.V. FAT-Schriftenreihe; 168)

[4] Majic N 2014 Entwicklung einer FEM-basierten Methode zur fertigungsorientierten Sickenmustergestaltung für biegebeanspruchte Tragstrukturen = Development of a FEM-based method for the design of production-oriented bead patterns for bending loaded support structures *PhD Thesis* Karlsruhe Institute of Technology

[5] Revfi S, Mikus M, Behdinan K and Albers A 2020 Bead optimization in long fiber reinforced polymer structures: Consideration of anisotropic material properties resulting from the manufacturing process *Advances in Engineering Software* **149** 102891

[6] Mock W 2004 *Das neue Dach des Airbus A380* https://www.ingenieur.de/technik/fachbereiche/raumfahrt/das-neue-dach-airbus-a380/ (accessed 22 Mar 2021)

[7] Monden A 2016 Adhäsion zwischen epoxidharzbasiertem CFK und oberflächenmodifiziertem Stahl: Grenzschichtversagen von Hybridlaminaten unter Mode I, Mode II und Mixed-Mode Belastung *PhD Thesis* University of Augsburg

[8] Cha W-G 2019 Formability consideration in bead optimization to stiffen deep drawn parts *PhD Thesis* Technical University of Munich

[9] Weinschenk A and Volk W 2017 FEA-based development of a new tool for systematic experimental validation of nonlinear strain paths and design of test specimens *AIP Conference Proceedings* **1896** 20009

[10] Wunderling C, Mayr L, Meyer S P and Zaeh M F 2020 Laser-based surface pre-treatment for metal-plastic hybrids using a new process strategy *Journal of Materials Processing Technology* **282** 116675